



# Activation analysis and waste management for blanket materials of multi-functional experimental fusion–fission hybrid reactor (FDS-MFX)

Jieqiong Jiang\*, Baoxin Yuan, Jun Zou, Yican Wu

*Institute of Nuclear Energy Safety Technology, Chinese Academy of Sciences, Hefei, Anhui 230031, China*



## ARTICLE INFO

### Article history:

Received 14 September 2012  
Received in revised form 19 March 2014  
Accepted 21 March 2014  
Available online 21 April 2014

**Keywords:**  
Fusion  
Fission  
Hybrid  
Multi-functional experimental reactor  
Blanket  
Activation

## ABSTRACT

The preliminary studies of the activation analysis and waste management for blanket materials of the multi-functional experimental fusion–fission hybrid reactor, i.e. Multi-Functional eXperimental Fusion Driven Subcritical system named FDS-MFX, were performed. The neutron flux of the FDS-MFX blanket was calculated using VisualBUS code and Hybrid Evaluated Nuclear Data Library (HENDL) developed by FDS Team. Based on these calculated neutron fluxes, the activation properties of blanket materials were analyzed by the induced radioactivity, the decay heat and the contact dose rate for different regions of the FDS-MFX blanket. The safety and environment assessment of fusion power (SEAPP) strategy, which was developed in Europe, was applied to FDS-MFX blanket for the management of activated materials. Accordingly, the classification and management strategy of activated materials after different cooling time were proposed for FDS-MFX blanket.

© 2014 Elsevier B.V. All rights reserved.

## 1. Introduction

An early application of fusion energy [1–14] can be achieved by the development of fusion–fission hybrid reactors. The Fusion Driven Subcritical System for Spent Fuel Blanket (FDS-SFB) is a conceptual hybrid fusion–fission reactor conceived for nuclear waste transmutation, fissile fuel breeding, tritium production and energy production. The fusion neutron source design is based on relatively easy-achievable plasma parameters. The parameters were extrapolated from the successful operation of the Experimental Advanced Superconducting Tokamak (EAST) in China as well as of other tokamaks operating in the world. The design of the sub-critical fissile blanket surrounding the tokamak is based upon the well-developed fission reactors technology. A hybrid reactor, i.e. the Fusion Driven Subcritical Multi-functional eXperimental reactor (FDS-MFX), has been proposed as a mid-term scenario by FDS Team [1,15–27]. It represents one scenario option for the China Fusion Engineering Test Reactor (CFETR) conceived for checking and validating the relevant viable fusion and fission technologies for both the pure fusion DEMO reactor and

the fusion–fission hybrid DEMO reactor (for Spent Fuel Burning).

Research and development of fusion–fission hybrid reactor materials, especially their activation characteristics, is one of the key issues for hybrid research in the world. The activation of the materials would substantially influence not only the safety of the fusion–fission hybrid reactors but also the recycling of used reactor materials and waste management. The selection of materials including structural material and tritium breeder is very important and effective method to control the neutron-induced activation on fusion reactors as well as to ensure the attractiveness of fusion–fission nuclear power regarding safety and environmental aspects.

In this study, the key activation analysis and waste management for blanket materials of the multi-functional experimental fusion–fission hybrid reactor FDS-MFX were estimated. The calculation and analysis of activation levels for different regions of FDS-MFX blanket, including radioactivity, decay heat and contact dose rate, were performed and used to analyze the activation properties of blanket materials. The safety and environment assessment of fusion power (SEAPP) [28] strategy, which was developed in Europe, was applied to FDS-MFX blanket for the management of activated materials. Finally, the classification and management strategy of activated materials after different cooling time were proposed for FDS-MFX blanket.

\* Corresponding author. Tel.: +86 551 65595392; fax: +86 551 65593681.  
E-mail address: [jieqiong.jiang@fds.org.cn](mailto:jieqiong.jiang@fds.org.cn) (J. Jiang).

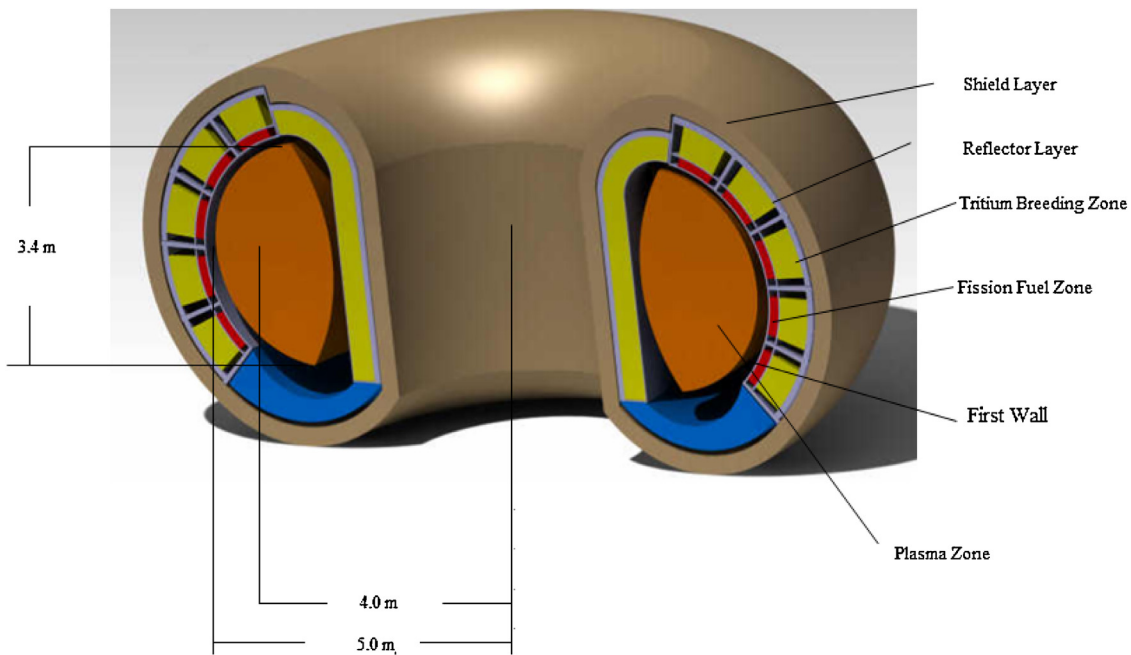


**Fig. 1.** Three-dimensional (3D) configuration of the helium-cooled blanket of FDS-MFX.

## 2. Codes, data libraries and calculation model

### 2.1. Codes and data libraries

In this study, the neutron flux of the FDS-MFX blanket was calculated using the last version of multi-functional neutronics analysis system VisualBUS [29–31] and the Hybrid Evaluated Nuclear Data Library (HENDL) [32,33], which were both developed by FDS Team. Based on these calculated neutron fluxes, the activation properties of blanket materials were analyzed by the induced radioactivity, the decay heat and the contact dose rate for different regions of the FDS-MFX blanket.

### 2.2. Calculation model

For accurate estimation, detailed three-dimensional (3D) neutronics models are needed. The proposed 3D configuration of the helium-cooled blanket can be seen in Fig. 1 and Ref. [34]. The major and minor radii of tokamak are 400 cm and 100 cm, respectively. The fusion power of the tokamak core is  $\sim 50$  mW, the power gain is  $\sim 1$ , the average neutron wall loading is  $\sim 0.17$  mW/m<sup>2</sup>, the elongation of plasma zone is  $\kappa = 1.7$ . The goal of FDS-MFX is to use subcritical blanket which interacts with the copious neutron source provided by fusion core to achieve tritium breeding and fission energy production. Besides the shielding modules, two types of functional blanket modules, Tritium Breeding Module (TBM) and Uranium Modules ((NUM (Natural Uranium Module) and HEUM (High Enriched Uranium Module), have been designed [34]. The function of inboard blanket is to breed tritium only while the outboard blanket is designated to produce energy with fission materials as well as breed tritium. The outboard blanket is Helium gas-Cooled plate fission fuel Blanket (named HCB) with additional Li<sub>17</sub>Pb<sub>83</sub> eutectic self-cooled tritium breeding zone. The low activation ferritic-martensitic steel (RAFM) e.g. the CLAM (China Low Activation Martensitic) [35–37] steel is employed as a candidate structural material.

The detailed 3D calculation model was automatically accomplished using MCAM [38]. MCAM is an interface program and integrated modeling system implementing the bi-directional

conversion between CAD model and MC simulation model; it supports a series of supplementary functions such as creation and repair of CAD model and analysis of physical properties.

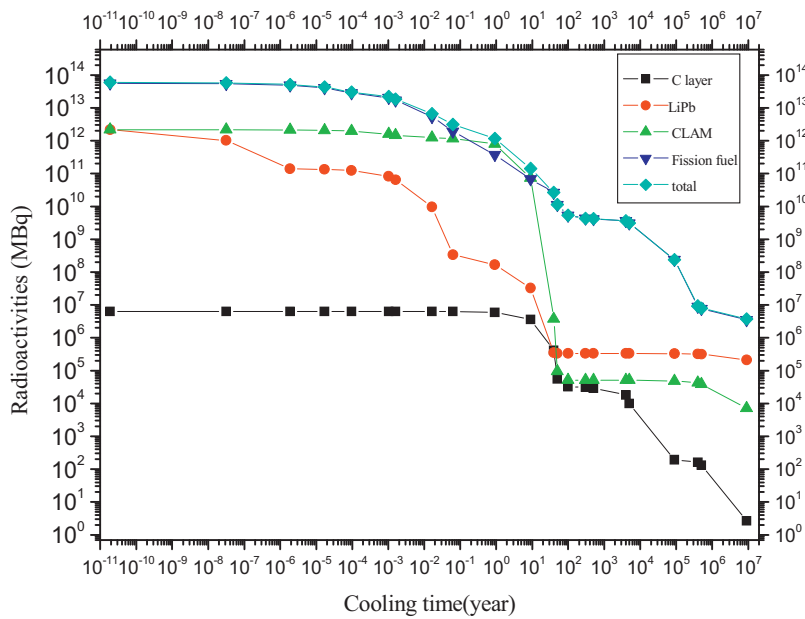
## 3. Results and analysis

### 3.1. Radioactivities

The materials irradiated by D-T high-energy neutrons for a prolonged time will suffer severe activation, which cannot be ignored. The radioactivity induced in the constituent materials of FDS-MFX Blanket by D-T fusion and fission neutron has been calculated. The two main aspects which are affecting the activation properties of HCB are considered: (1) neutron irradiation conditions (flux, and irradiation time, etc.: the flux was based on the reference neutronics design of the FDS-MFX blanket, the total flux of HCB was about  $9.0 \times 10^{13}$  (1/cm<sup>2</sup> s), which can be seen in Ref. [34]; the total accumulated irradiation time for the NUM and HEUM are 5 years and 3 years, respectively). (2) Types of irradiated materials: carbon (C) layer, Li<sub>17</sub>Pb<sub>83</sub> (LiPb), CLAM, fission fuel, etc.

The total activity of the whole blanket and the activities of the typical zones as a function of cooling time of the FDS-MFX blanket are shown in Fig. 2. At the shutdown, the total activity of the FDS-MFX blanket is  $6.03 \times 10^{13}$  MBq, which is mainly induced by the activation of the fission fuel, Li<sub>17</sub>Pb<sub>83</sub>, and CLAM. The activities in the typical zones after shutdown with different cooling times can be found in Table 1. The activity of the fission fuel is of the highest value (92.7% of the total activity).

The activity induced in the fission fuels decays very slowly (from  $5.59 \times 10^{13}$  MBq to  $5.34 \times 10^9$  MBq during the first 100 years). Because of the high-level fission products and actinides, the activity after 100 years' cooling is  $5.34 \times 10^9$  MBq, which is the 0.0089% of the activity at the beginning of shutdown, but the activity is still strong. The total activity of FDS-MFX blanket after 100 years' cooling is almost near to the activity of the fission fuel. Moreover, the total activities of the blanket after 500 years', 5000 years', 90,000 years', and 500,000 years' cooling are  $4.19 \times 10^9$  MBq,  $3.14 \times 10^9$  MBq,  $2.39 \times 10^8$  MBq, and  $7.67 \times 10^6$  MBq, respectively.

**Fig. 2.** Activities in the typical zones after shutdown as a function of cooling time.**Table 1**

The activities in the typical zones after shutdown with different cooling times.

Cooling time (a)	C Layer (MBq)	LiPb (MBq)	CLAM (MBq)	Fission fuel (MBq)	Total FDS-MFX blanket (MBq)
0	6.32E+06	2.17E+12	2.19E+12	5.59E+13	6.03E+13
100	3.21E+04	3.32E+05	5.16E+04	5.34E+09	5.34E+09
500	2.91E+04	3.32E+05	5.14E+04	4.20E+09	4.20E+09
5000	9.88E+03	3.32E+05	5.10E+04	3.14E+09	3.14E+09
90,000	1.95E+02	3.31E+05	4.89E+04	2.40E+08	2.40E+08
500,000	1.32E+02	3.18E+05	3.87E+04	7.68E+06	8.03E+06

The activation level of the tritium breeder  $\text{Li}_{17}\text{Pb}_{83}$ , is mainly due to Pb under the condition that tritium contribution has been ignored since there is a little contribution (0.0007%) of Li activation to  $\text{Li}_{17}\text{Pb}_{83}$ . At shutdown time, the activation level of the tritium breeder  $\text{Li}_{17}\text{Pb}_{83}$ , is dominated by the nuclides  $\text{Pb-207m}$  ( $T_{1/2} = 0.8$  s), which are mainly produced via the reactions  $\text{Pb-208(n, 2n)}$ ,  $\text{Pb-207m}$  and  $\text{Pb-207(n, n')Pb-207m}$ , and  $\text{Pb-207m}$  that decays very fast. A few minutes later, the activation level of  $\text{Li}_{17}\text{Pb}_{83}$  is dominated by the nuclide  $\text{Pb-204m}$  ( $T_{1/2} = 66.9$  min) up to  $\sim 2$  h after shutdown. From  $\sim 2$  h to  $\sim 60$  days after shutdown, the nuclides  $\text{Pb-203}$  ( $T_{1/2} = 52.1$  h) and  $\text{Tl-202}$  ( $T_{1/2} = 12$  days) dominate the total activity of  $\text{Li}_{17}\text{Pb}_{83}$ . Then the total activity of  $\text{Li}_{17}\text{Pb}_{83}$  is mainly due to the nuclide  $\text{Bi-207}$  ( $T_{1/2} = 31.8$  years) up to  $\sim 250$  years after shutdown. After that time, the total activity of  $\text{Li}_{17}\text{Pb}_{83}$  is dominated by the nuclide  $\text{Ag-108m}$  ( $T_{1/2} = 438$  years) up to  $\sim 1000$  years after shutdown. The nuclide  $\text{Bi-208}$  ( $T_{1/2} = 3.7 \times 10^5$  years) becomes the dominant nuclide for the total activity of  $\text{Li}_{17}\text{Pb}_{83}$  thereafter. These dominant nuclides are produced during the irradiation process by different nuclides.

The specific activity of the blanket after 50 years' cooling is  $5.6 \times 10^5$  Bq/kg, which is low to control the long-term level of the activity [39].

The activation level of the CLAM is dominated by the nuclide  $\text{Fe-55}$  ( $T_{1/2} = 2.6$  y),  $\text{Mn-56}$  ( $T_{1/2} = 2.58$  h), and  $\text{W-187}$  ( $T_{1/2} = 23.85$  h). The activities due to minor elements (trace elements) could dominate after long cooling time [39]. The trace elements had been taken into account in materials composition used in these calculations, for example, the trace elements such as Co, Nb, Mo, Ni and so on had been included in related calculation of the CLAM [40]. At the shutdown, the activity of CLAM decrease slowly (from  $2.19 \times 10^{12}$  MBq to  $7.91 \times 10^{11}$  MBq during the first 1 year), the total activity after 1 year's cooling is  $7.91 \times 10^{11}$  MBq, after the activity decreases more quickly becoming  $5.16 \times 10^4$  MBq after  $\sim 100$  years' cooling, the specific activity of the blanket after 50 years' cooling is  $2.92 \times 10^6$  Bq/kg which is low to the controlled long-term level of the activity [41].

### 3.2. Decay heat

Let consider NUM and HEUM and let assume they are irradiated for 5 and 3 years according to the blanket design, respectively. The calculated decay heat versus cooling time of their constituent materials (C layer,  $\text{Li}_{17}\text{Pb}_{83}$ , CLAM, fission fuel, etc.) is plotted in Fig. 3. To note that in the calculation tritium production has been ignored.

**Table 2**

The decay heat in the typical zones after shutdown with different cooling times.

Cooling time (a)	C Layer (kW)	LiPb (kW)	CLAM (kW)	Fission Fuel (kW)	Total FDS-MFX blanket (kW)
0	5.96E-06	5.34E+02	2.13E+02	9.96E+03	1.07E+04
100	2.58E-07	3.66E-06	1.77E-07	2.24E+00	2.24E+00
5000	8.40E-08	3.66E-06	1.66E-07	1.34E+00	1.34E+00
500,000	5.27E-09	3.47E-06	3.07E-08	4.23E-03	4.23E-03

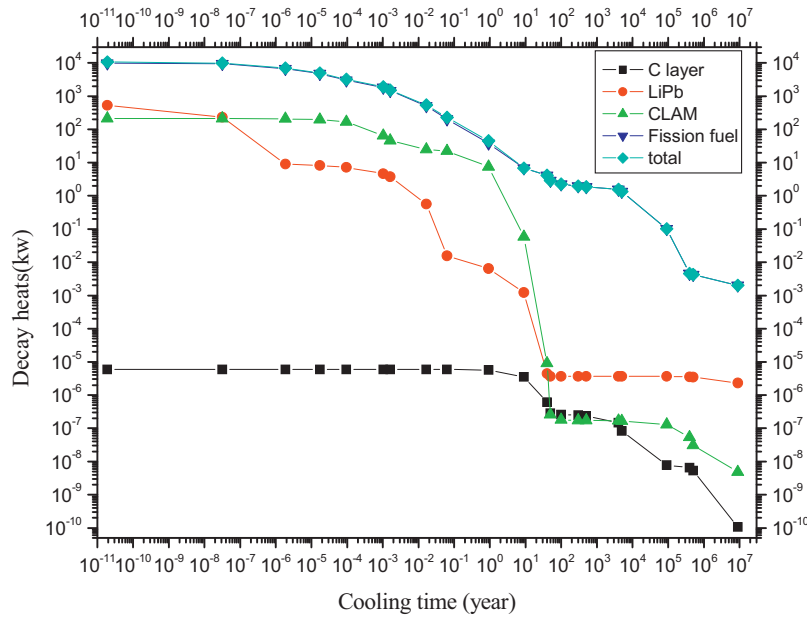


**Fig. 3.** Decay heats in typical zones after shutdown as a function of cooling time.

The corresponding after shutdown decay heat versus cooling time is reported in Table 2.

At the shutdown, the total decay heat of the FDS-MFX blanket is 10.71 mW. The percentages of the fission fuel,  $\text{Li}_{17}\text{Pb}_{83}$ , and CLAM in the total decay heat are 93.02%, 4.99%, and 1.99%, respectively. The decay heat of C layer is very low and has been ignored in the analysis. The decay heat of FDS-MFX blanket is mainly produced by the large amounts of high-level fission products and actinides. At the shutdown, the decay heat decreases quickly (from  $1.07 \times 10^4$  kW to 0.54 mW during the first week); the total decay heat of the blanket after 1 week's cooling reduces to 0.54 mW. Then the decay heat decreases slowly than that in the first week, and for cooling time of 100 years', 5000 years', and 500,000 years', it is 2 kW, 1 kW, and 4.2 W, respectively. At the shutdown, the decay heat of  $\text{Li}_{17}\text{Pb}_{83}$  which is dominated by decay of the nuclide Pb-207m ( $T_{1/2} = 0.8$  s) is slightly higher than that of CLAM, then it reduces very quickly with

the rapid decay of Pb-207m. After ~50 years' cooling the decay heat is reduced to  $3.66 \times 10^{-3}$  W, which is very small and can be ignored.

The decay heat of CLAM is dominated by the nuclides Mn-56 ( $T_{1/2} = 2.58$  h), W-187 ( $T_{1/2} = 23.85$  h) and Ta-182 ( $T_{1/2} = 114$ d), which are mainly produced via the reactions Mn-55( $n,\gamma$ ) Mn-56, W-186( $n,\gamma$ ) W-187 and Ta-181( $n,\gamma$ )Ta-182. At the shutdown, the decrease of the decay heat of CLAM is slow after 1 year's cooling, and then it becomes very fast, the total decay heat after 50 years' cooling is  $1.77 \times 10^{-4}$  W.

Moreover, residual heat removal system and storage strategy of nuclear waste need to be designed according to the variation of decay heat, the safety of thermal hydraulics will be affected by the power density of the decay heat. In this study, the decay heat power densities in the NUM and HEUM after shutdown have been analyzed as a function of cooling time. The decay heat power densities in the NUM and HEUM after shutdown can be found in Fig. 4.

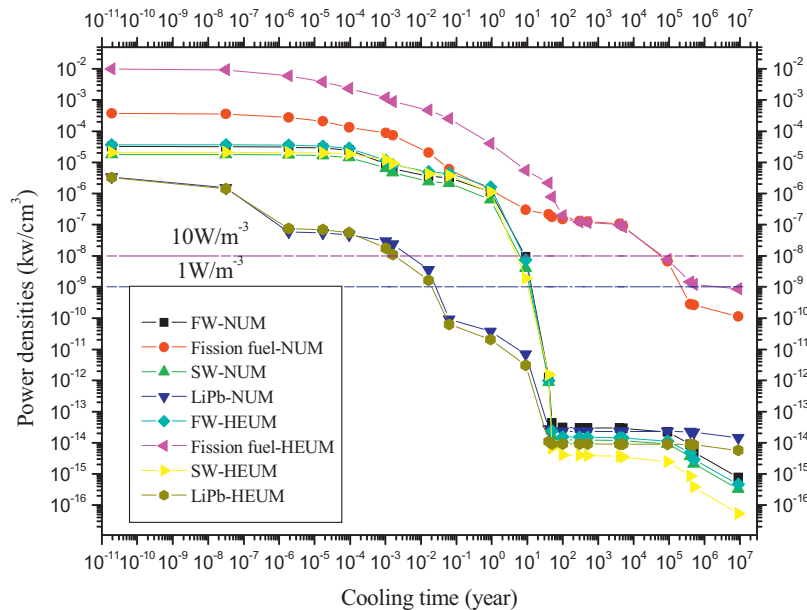


**Fig. 4.** Decay heat power densities in the NUM and HEUM after shutdown as a function of cooling time.

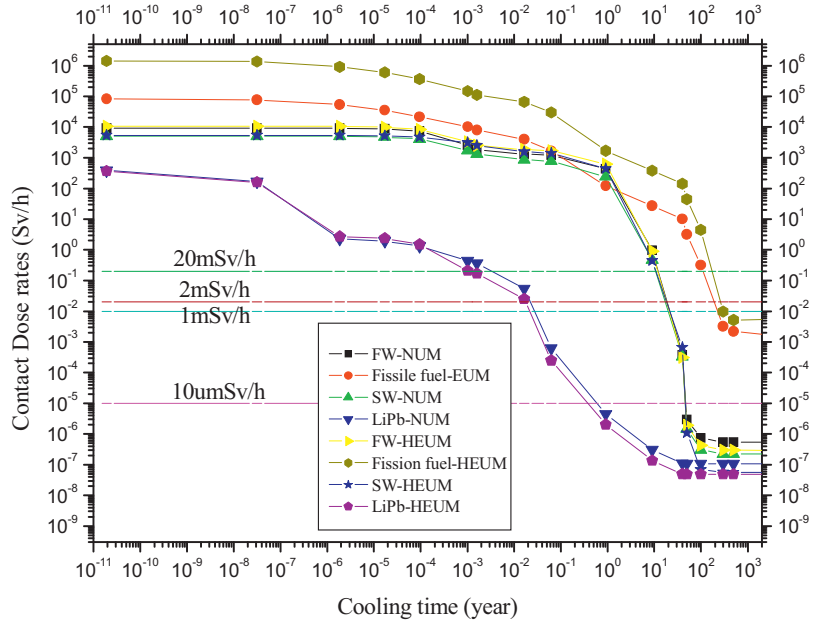


**Fig. 5.** Contact dose rates in the NUM and HEUM after shutdown as a function of cooling time.

The more initial loading of fission fuel and the higher neutron flux in the HEUM, the more fission products and actinides is produced in the HEUM, as a result the decay heat power density of the fission fuel is much higher in the HEUM than that in the NUM. Due to the existence of the high-level fission products and actinides, the decrease of the decay heat power densities in the both type's models are slow. The decay heat power densities of the fission fuel in the NUM and HEUM after 100 years' cooling are  $196 \text{ W/m}^3$  and  $148 \text{ W/m}^3$ , respectively.

The difference of decay heat power densities of CLAM between NUM and HEUM is quite small over the whole cooling time. At the shutdown, the decay heat power density of CLAM in the NUM and HEUM is  $\sim 0.01 \text{ mW/m}^3$ . The decay heat power density of CLAM in the First Wall (FW) of the HEUM is little higher than that of the NUM. And for CLAM in the Structural Wall (SW), the decay heat power density is lower than that of the CLAM in the FW due to lower neutron flux. At the shutdown, the decrease of the decay heat power density is slow, then the decrease of the decay heat becomes very fast, the average decay heat power density after 50 years' cooling is  $\sim 1.0 \times 10^{-5} \text{ W/m}^3$ , which is lower than the simple recycle material limit of  $<1 \text{ W/m}^3$  [28].

As shown in Fig. 4, at the shutdown, the decay heat power densities of the  $\text{Li}_{17}\text{Pb}_{83}$  in the NUM and HEUM are  $3.24 \text{ kW/m}^3$  and  $3.41 \text{ kW/m}^3$ , respectively. The decrease trend of the decay heat power density of  $\text{Li}_{17}\text{Pb}_{83}$  in the NUM is in accordance with that of the  $\text{Li}_{17}\text{Pb}_{83}$  in the HEUM during the cooling time. The decay heat power density of the  $\text{Li}_{17}\text{Pb}_{83}$  is dominated by the activation level of the  $\text{Li}_{17}\text{Pb}_{83}$  (note that tritium has been ignored). The decay heat power densities of the  $\text{Li}_{17}\text{Pb}_{83}$  in the NUM and HEUM after 1 year's cooling are  $0.02 \text{ W/m}^3$  and  $0.037 \text{ W/m}^3$ , respectively, which will be lower than simple recycle material limit of  $1 \text{ W/m}^3$ . And the decay heat of C layer is very small ( $\leq 5.96 \times 10^{-6} \text{ kW}$ ), which has been ignored in the analysis.

### 3.3. Contact dose rates

As a function of cooling time, the contact dose rates in the NUM and HEUM after shutdown can be found in Fig. 5. The contact dose rate of the fission fuel in the HEUM is much higher than that of the fission fuel in the NUM, the explanation of this point can be the

same as for activity. Due to the existence of the high-level fission products and actinides, the decrease of the contact dose rates in both type's models are slow. The contact dose rates of the fission fuel in the NUM and HEUM after 500 years' cooling are  $5 \text{ mSv/h}$  and  $2 \text{ mSv/h}$ , respectively, which are lower than the limitation level of complex recovery processing ( $<20 \text{ mSv/h}$ ) [42], but still higher than the limitation level of simple recovery processing ( $<10 \mu\text{Sv/h}$ ) [43].

The difference of contact dose rate of CLAM between NUM and HEUM is quite small during the cooling time. The contact dose rate of CLAM is dominated by the nuclide Mn-56 ( $T_{1/2} = 2.58 \text{ h}$ ), W-187 ( $T_{1/2} = 23.85 \text{ h}$ ), and Ta-182 ( $T_{1/2} = 114 \text{ d}$ ). At the shutdown, the contact dose rate is  $\sim 10^4 \text{ Sv/h}$ , the decrease of the contact dose rate is slow (from  $\sim 10^4 \text{ Sv/h}$  to  $6.2 \times 10^2 \text{ Sv/h}$  in the first year), then it becomes very fast (from  $6.2 \times 10^2 \text{ Sv/h}$  to  $4.27 \times 10^{-7} \text{ Sv/h}$ ) after  $\sim 1$  year's to  $\sim 100$  years' cooling. The contact dose rates of CLAM of the NUM and HEUM are both less than  $3 \mu\text{Sv/h}$ , which are lower than hands-on recycling limit  $10 \mu\text{Sv/h}$  [42].

From Fig. 5 it can be seen that the decrease of the contact dose rate of  $\text{Li}_{17}\text{Pb}_{83}$  in the NUM is in accordance with that of the  $\text{Li}_{17}\text{Pb}_{83}$  in the HEUM during the cooling time. The contact dose rate of the  $\text{Li}_{17}\text{Pb}_{83}$  is dominated by the activation level of the  $\text{Li}_{17}\text{Pb}_{83}$  (note that tritium has been ignored). The contact dose rates of the LiPb in the NUM and HEUM after 1 year's cooling are,  $4.5 \mu\text{Sv/h}$  and  $2.5 \mu\text{Sv/h}$ , respectively. Which are lower than hands-on recycling limit of  $10 \mu\text{Sv/h}$ .

### 3.4. Nuclear waste assessment

The safety and environment assessment of fusion power (SEAFP) strategy, which was developed in Europe, was applied to the management of activated materials for FDS-MFX blanket. Activation analysis was based on the irradiation time of 5 years and 3 years for NUM and HEUM respectively. For the assessment of the waste, the following conditions were assumed: all the activated components of the FDS-MFX blanket have been done with detritiation processes, and all the tritium in the nuclear waste, including the bred tritium and the permeated tritium, has been removed.

The classification and management strategy of activated materials for FDS-MFX blanket after 50 years' and 100 years' cooling was proposed based on above analysis as shown in Table 3. From

**Table 3**

Proposed activated materials classification and management strategy of FDS-MFX blanket.

Materials	50 years' strategy	100 years' strategy	Mass/t
CLAM	SRM (HOR)	SRM (HOR)	35.1
$\text{Li}_{17}\text{Pb}_{83}$	SRM (HOR)	SRM (HOR)	1124
Fission fuel in NUM	PDW	PDW	23.6
Fission fuel in HEUM	PDW	PDW	2.17
C layer	SRM (HOR)	SRM (HOR)	34.3

data of **Table 3** it can be assumed that after 50 years cooling time, the activated CLAM,  $\text{Li}_{17}\text{Pb}_{83}$  and C will be low activity level material. This allows to consider them to be done by hand-on recycling (HOR) as simple recycle materials (SRM). After 100 years cooling, the activated fission fuel is still high-level radioactive waste and cannot be considered to be recycled as permanent disposal waste (PDW). A solution can be to further burn the FDS-MFX fission fuel in an advanced nuclear energy system such as a sub-critical system (e.g. fusion–fission hybrid DEMO reactor or in an accelerator-driven system). This option is to be evaluated on the basis of the best and safe environmental impact.

#### 4. Conclusions

Using a home-developed code VisualBUS and the Hybrid Evaluated Nuclear Data Library HENDL, the calculation and analysis of activation levels for different regions of FDS-MFX blanket, including radioactivity, decay heat and contact dose rate, were calculated and used to analyze the activation properties of blanket materials. The classification and management strategy of activated materials for FDS-MFX blanket after different cooling time were proposed.

- (1) The activity and decay heat of the helium-cooled blanket of FDS-MFX are mainly produced by fissile fuel. At the shutdown, the total activity and decay heat of the FDS-MFX blanket are  $6.03 \times 10^{13} \text{ MBq}$  and  $10.71 \text{ mW}$ , respectively. The activation and the decay heat of the CLAM (China Low Activation Martensitic) and tritium breeding material  $\text{Li}_{17}\text{Pb}_{83}$  are reduced during the cooling time from 1 year to 100 years. The activation level ( $5.6 \times 10^5 \text{ Bq/kg}$ ) and the decay heat ( $3.66 \times 10^{-3} \text{ W}$ ) of tritium breeder  $\text{Li}_{17}\text{Pb}_{83}$  after 50 years' cooling is low to the controlled long-term level.
- (2) The decay heat power density of the fission fuel in the HEUM (High Enriched Uranium Module) is much higher than that of the fission fuel in the NUM (Natural Uranium Module). At the shutdown, the decay heat power densities of the fission fuel in the HEUM and NUM are  $10 \text{ mW/m}^3$  and  $0.37 \text{ mW/m}^3$ , respectively. Due to the existence of high-level fission products and actinides, the decrease of the decay heat power densities in both type's models are slow.
- (3) The difference of decay heat and contact dose rate of CLAM between NUM and HEUM are quite small during the cooling time. The decrease of the contact dose rate is slow since it passes from  $\sim 10^4 \text{ Sv/h}$  at shut down to  $6.2 \times 10^2 \text{ Sv/h}$  after  $\sim 1$  year'. After the dose rate decreases more quickly becoming  $4.27 \times 10^{-7} \text{ Sv/h}$  after  $\sim 100$  years' cooling. It worth to note that after 50 years' cooling, the average decay heat power density is  $\sim 1.0 \times 10^{-5} \text{ W/m}^3$ , which is already lower than the limitation level of recovery processing ( $< 1 \text{ W/m}^3$ ). The contact dose rates of CLAM of NUM and HEUM are both less than  $3 \mu\text{Sv/h}$ , which are lower than hands-on recycling limit of  $10 \mu\text{Sv/h}$ .
- (4) The decrease trends of the decay heat and the contact dose rate of  $\text{Li}_{17}\text{Pb}_{83}$  in the NUM are in accordance with those of the  $\text{Li}_{17}\text{Pb}_{83}$  in the HEUM during the cooling time. The decay heat power density of the  $\text{Li}_{17}\text{Pb}_{83}$  in the NUM and HEUM after 1 and 100 year's cooling are  $0.02 \text{ W/m}^3$  and  $0.037 \text{ W/m}^3$ , respectively.

These values will be lower than simple recycle material limit of  $1 \text{ W/m}^3$ . The contact dose rates of the  $\text{Li}_{17}\text{Pb}_{83}$  in the NUM and HEUM after 1 year's cooling are  $4.5 \mu\text{Sv/h}$  and  $2.5 \mu\text{Sv/h}$ , respectively, which are lower than hands-on recycling limit of  $10 \mu\text{Sv/h}$ .

- (5) The proposed classification and management strategy of activated materials for FDS-MFX blanket after 50 and 100 years' cooling time was based upon the safety and environment assessment of fusion power (SEAFP) strategy. After 50 years' cooling, the activated CLAM,  $\text{Li}_{17}\text{Pb}_{83}$  and C will be low activity level material, and can be considered to be done, by hand-on recycling (HOR) as simple recycle materials (SRM). The activated fission fuel in the FDS-MFX blanket is still high-level radioactive waste after 100 years' cooling, which cannot be recycled as permanent disposal waste (PDW). The blanket of FDS-MFX can also benefit from nuclear fuel disposal loaded with nuclear waste for transmutation in the future.

#### Acknowledgments

This work was supported by the China National Natural Science Foundation with Grant Nos. 51001095 and 50901072, the Important Direction Program of Chinese Academy of Sciences with Grant No. KJCX2-YW-N35. We would like to thank the great help from the members of FDS Team in this research.

#### References

- [1] Y. Wu, J. Jiang, M. Wang, M. Jin, FDS Team, A fusion-driven subcritical system concept based on viable technologies, Nucl. Fusion 51 (2011), <http://dx.doi.org/10.1088/0029-5515/51/10/103036>.
- [2] H.A. Bethe, The fusion hybrid, Phys. Today 5 (1979) 44–51.
- [3] B.R. Leonard Jr., A review of fusion–fission (hybrid) concepts, Nucl. Technol. 20 (1973) 161–178.
- [4] S.I. Abdel-Khalik, P. Jansen, G. Kessler, P. Klumpp, Impact of fusion–fission hybrids on world nuclear future, Atomk. Kerntechnik 38 (1981) 1–11.
- [5] D.H. Berwald, J. Maniscalco, An economics method for symbiotic fusion–fission electricity generator systems, Nucl. Technol. Fusion 1 (1981) 128–137.
- [6] E.T. Cheng, R.J. Cerbone, Prospect of nuclear waste transmutation and power production in fusion reactors, Fusion Technol. 30 (1996) 1654–1658.
- [7] M. Salvatores, Physics features comparison of TRU burners fusion/fission hybrids accelerator-driven systems and low conversion ratio critical fast reactors, Ann. Nucl. Energy 36 (11/12) (2009) 1653–1662.
- [8] Y. Gohar, Fusion solution to dispose of spent nuclear fuel, transuranic elements, and highly enriched uranium, Fusion Eng. Des. 58/59 (2001) 1097–1101.
- [9] A. Serikov, G. Shatalov, S. Sheludjakov, Y. Shpansky, N. Vasiliev, Possibility of fusion power reactor to transmute minor actinides of spent nuclear fuel, Fusion Eng. Des. 63/64 (2002) 93–99.
- [10] W.M. Stacey, J. Mandrekas, E.A. Hoffman, G.P. Kessler, C.M. Kirby, A.N. Mauer, et al., A fusion transmutation of waste reactor, Fusion Eng. Des. 63/64 (2002) 81–86.
- [11] S. Sahin, M. Ubuyli, LWR spent fuel transmutation in a high power density fusion reactor, Ann. Nucl. Energy 31 (2004) 871–890.
- [12] I. Murata, Y. Yamamoto, S. Shido, K. Kondo, A. Takahashi, E. Ichimura, et al., Fusion-driven hybrid system with ITER model, Fusion Eng. Des. 75–79 (2005) 871–875.
- [13] D. Ridikas, R. Plukis, A. Plukis, E.T. Cheng, Fusion–fission hybrid system for nuclear waste transmutation (I): characterization of the system and burn-up calculations, Prog. Nucl. Energy 48 (2006) 235–246.
- [14] W.M. Stacey, Transmutation missions for fusion neutron sources, Fusion Eng. Des. 82 (2007) 11–20.
- [15] Y. Wu, FDS Team, Conceptual design activities of FDS series fusion power plants in China, Fusion Eng. Des. 81 (2006) 2713–2718.
- [16] Y. Wu, S. Zheng, X. Zhu, W. Wang, H. Wang, S. Liu, et al., Conceptual design of the fusion-driven subcritical system FDS-I, Fusion Eng. Des. 81 (2006) 1305–1311.
- [17] Y. Wu, FDS Team, Conceptual design activities of FDS series fusion power plants in China, Fusion Eng. Des. 81 (2006) 2713–2718.
- [18] Y. Wu, Progress in fusion-driven hybrid system studies in China, Fusion Eng. Des. 63/64 (2002) 73–80.
- [19] Y. Wu, A fusion neutron source driven sub-critical nuclear energy system: a way for early application of fusion technology, Plasma Sci. Technol. 3 (6) (2001) 1085–1092.
- [20] Y. Wu, L. Qiu, Y. Chen, Conceptual study on liquid metal center conductor post in spherical tokamak reactors, Fusion Eng. Des. 51/52 (2000) 395–399.
- [21] L. Qiu, Y. Wu, B. Xiao, Q. Xu, Q. Huang, B. Wu, et al., A low aspect ratio tokamak transmutation system, Nucl. Fusion 40 (3) (2000) 629–633.

- [22] Y. Wu, FDS Team, Conceptual design of the China fusion power plant FDS-II, *Fusion Eng. Des.* 83 (2008) 1683–1689.
- [23] H. Chen, Y. Wu, S. Konishi, J. Hayward, A high temperature blanket concept for hydrogen production, *Fusion Eng. Des.* 83 (2008) 903–911.
- [24] Y. Wu, B. Xiao, Q. Huang, L. Qiu, Neutron radiation effects of the center conductor post in a low aspect ratio tokamak reactor, *J. Nucl. Mater.* 258–263 (1998) 339–344.
- [25] Y. Wu, FDS Team, Conceptual design and testing strategy of a dual functional lithium–lead test blanket module in ITER and EAST, *Nucl. Fusion* 47 (11) (2007) 1533–1539.
- [26] Y. Wu, J. Jiang, H. Chen, S. Liu, Y. Bai, Y. Chen, et al., The Fusion–Fission Hybrid Reactor for Energy Production: A Practical Path to Fusion Application, in: 22nd Int. Conf. Fusion Energy (FEC-22) (Geneva, Switzerland, October, 2008) FT/P 3-21, International Atomic Energy Agency, Vienna, 2008.
- [27] Y. Wu, J. Jiang, M. Wang, M. Jin, Z. Chen, J. Liu, et al., Re-Evaluation of Fusion–Fission Hybrid Reactors for Energy Production, Fuel Breeding and Waste Transmutation, in: Presentation at the 3rd IAEA Technical Meeting on First Generation of Fusion Power Plants Design and Technology, Vienna, Austria, July 13–15, 2009.
- [28] P. Rocco, M. Zucchetti, Recycling and clearance possibilities-final report of task 4.2, SEAFP2:4.2; JRC:4 (Rev.1), 1998.
- [29] Y. Wu, J. Li, Y. Li, Q. Zeng, M. Chen, S. Zeng, et al., An integrated multi-functional neutronics calculation and analysis code system: VisualBUS, *Chin. J. Nucl. Sci. Eng.* 27 (2007) 365–373.
- [30] Y. Wu, FDS Team, CAD-based interface programs for fusion neutron transport simulation, *Fusion Eng. Des.* 84 (2009) 1987–1992.
- [31] Y. Wu, Z. Xie, Ulrich Fischer a discrete ordinates nodal method for one-dimensional neutron transport numerical calculation in curvilinear geometries, *Nucl. Sci. Eng.* 133 (1999) 350–357.
- [32] J. Jiang, D. Xu, S. Zheng, Z. He, Y. Hu, J. Li, et al., Integral data benchmark of HENDL2.0/MG compared with neutronics shielding experiments, *Plasma Sci. Technol.* 11 (2009) 625–631.
- [33] J. Zou, Q. Zeng, D. Xu, L. Hu, P. Long, Design and production of fine-group cross section library HENDL3.0/FG for subcritical system, in: Proceeding of PHYSOR 2012 – Advances in Reactor Physics, Knoxville, TN, USA, April 15–20, 2012.
- [34] J. Jiang, B. Yuan, M. Jin, M. Wang, P. Long, L. Hu, Three-dimensional neutronics optimization of helium-cooled blanket for multi-functional experimental fusion–fission hybrid reactor (FDS-MFX), in: Proceeding of PHYSOR 2012 – Advances in Reactor Physics, Knoxville, TN, USA, April 15–20, 2012.
- [35] Q. Huang, C. Li, Y. Li, M. Chen, M. Zhang, L. Peng, et al., Progress in development of China low activation martensitic steel for fusion application, *J. Nucl. Mater.* 367–370 (2007) 142–146.
- [36] Y.C. Wu, J.P. Qian, J.N. Yu, The fusion-driven hybrid system and its material selection, *J. Nucl. Mater.* 307–311 (2002) 1629–1636.
- [37] Y. Wu, FDS Team, Fusion-based hydrogen production reactor and its material selection, *J. Nucl. Mater.* 386–388 (2009) 122–126, Also invited presentation at the 13th International Conference on Fusion Reactor Materials (ICFRM-13), December 10–14, 2007, Nice, France.
- [38] Y. Li, L. Lu, A. Ding, H. Hu, Q. Zeng, S. Zheng, et al., Benchmarking of MCAM4.0 with the ITER 3D model, *Nucl. Eng. Des.* 82 (2007) 2867–2871.
- [39] W. Pohorecki, S. Taczanowski, M. Kopec, et al., Activation, decay heat and waste analysis for a European HCLL DEMO concept, *Fusion Eng. Des.* 86 (2011) 2705–2708.
- [40] Q. Huang, J. Li, Y. Chen, Study of irradiation effects in China low activation martensitic steel CLAM, *J. Nucl. Mater. A* 329–333 (2004) 268–272.
- [41] The State Environmental Protection Administration (SEPA), 2002, the manager of the radioactive waste.
- [42] E.T. Cheng, D.K. Sze, J.A. Sommer, O.T. Farmer, Materials recycling, considerations for D-T fusion reactions, *Fusion Sci. Technol.* 21 (1992) 2001–2008.
- [43] T.J. Dolan, G.J. Butterworth, Vanadiumrecycling, *Fusion Technol.* 26 (1994) 1014–1020.